

CST0006

Numerical Analysis of Water Infiltration and Heat Transfer in Rectangular Porous Packed Bed

Sauce Aksornkitti, Somsak Vongpradubchai and Phadungsak Rattanadecho*

Center of Excellence in Electromagnetic Energy Utilization in Engineering (CEEE.)

Department of Mechanical Engineering, Faculty of Engineering

Thammasat University (Rangsit Campus), 99 moo 18, Klong Luang, Pathum Thani 12120, Thailand

*Corresponding Author: E-mail: ratphadu@engr.tu.ac.th, Tel.: +66-(0)-2564-3001 ext. 3153, fax: +66-(0)-2564-3010

Abstract

The characteristics of heat transfer and water infiltration in a rectangular porous packed bed due to supplied hot water are numerically study. The study is focus on the two-dimensional unsaturated flow in a porous packed bed column assuming local thermal equilibrium between water and solid matrix at any specific space. This numerical study described the dynamics of heat transfer and water infiltration in various testing conditions. Numerically, the influence of particle sizes on heat transfer and water infiltration during unsaturated flow is clarified in details. The results presented here can be basically used for analysis of numerous other applications (e.g. heat and water movement in the ground).

Keywords: Water infiltration, Temperature distribution, Rectangular porous packed bed.

1. Introduction

Understanding of heat transfer in porous packed bed or porous media with water infiltration due to the force of capillary action is essential in a variety of soil science and chemical engineering applications such as temperature control of soil, recovery of geothermal energy, thermal energy storage, and various reactors in the chemical industry. Up to the present time, the related problem of water infiltration in porous media has been investigated both experimentally and numerically by many researchers [1-8]. However, few research reports have been published for a coupled heat transfer with water infiltration in porous media, except the problem of permafrost [9-11], drying technology [12-16] and 1-D unsaturated flow with heat transfer in cylindrical porous media by our group [17-19].

The purpose of this paper is to clarify the characteristics of heat transfer with water infiltration in Rectangular Porous Packed Bed (next time will refer to RPP) numerically. Most importantly, the effect of particle sizes on the flow kinetics is numerical investigation. The result presented here provides a basis for fundamental understanding of heat transfer and water infiltration in porous media.

2. Numerical Analysis of Water Infiltration and Heat Transfer in Rectangular Porous Packed Bed

Fig.1 shows the physical models for heat transfer and water infiltration in RPP. This study case is focus on the unsaturated flow in porous packed bed due to supplied hot water. When the hot water is uniformly supplied at the top surface of the RPP, which is initially composed of glass particles and gas, a two-phase region with the infiltration front is formed within the packed bed. In this region, the only flow of liquid water is considered and gradient of gas pressure

is assumed to be neglected. However, the flow due to gas phase is a dominant mechanism at the lower part.

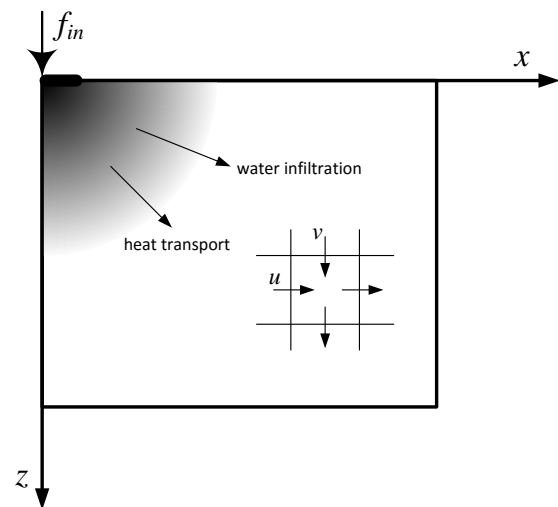


Fig. 1 Physical models for heat transfer and water infiltration in RPP

By conservation of mass and energy in the unsaturated porous packed bed, the governing equation of mass and energy for specified phase can be derived by using a volume averaged technique [16, 21]. The main transport mechanisms that enables water infiltration during supplied hot water into the RPP are capillary pressure gradient and gravity.

Assumptions

The main assumptions involved in the formulations of the transport model are:

- 1) The rectangular porous packed bed is rigid.
- 2) No chemical reactions occur in the rectangular porous packed bed.

CST0006

- 3) Local thermodynamic equilibrium is assumed.
- 4) Darcy's law holds for the liquid and gas phases.
- 5) Gravity is included for the flow analysis.
- 6) Gas pressure gradient inside porous packed bed is neglected.

Mass Conservation

The microscopic mass conservation equation for liquid phase is expressed respectively [16, 20], as shown below:
Liquid phase

$$\varepsilon \frac{\partial}{\partial t} [\rho_l s] = \frac{\partial}{\partial z} \left[\frac{KK_{rl}}{v_l} \left(\frac{\partial p_c}{\partial z} - \rho_l g \right) \right] + \frac{\partial}{\partial x} \left[\frac{KK_{rl}}{u_l} \left(\frac{\partial p_g}{\partial x} - \frac{\partial p_c}{\partial x} \right) \right] \quad (1)$$

According to the assumption 6); the Eq. (1) can be reduced as follows:

$$\varepsilon \frac{\partial}{\partial t} [\rho_l s] = \frac{\partial}{\partial z} \left[\frac{KK_{rl}}{v_l} \left(\frac{\partial p_c}{\partial z} - \rho_l g \right) \right] + \frac{\partial}{\partial x} \left[\frac{KK_{rl}}{u_l} \left(\frac{\partial p_c}{\partial x} \right) \right] \quad (2)$$

where ρ is density, s is water saturation, K is permeability, K_r is relative permeability, p is pressure, g is gravitational acceleration, v is velocity in z-axis, u is velocity in x-axis

Energy Equation

Ignoring kinetic energy and pressure terms which are usually unimportant, this can be obtained from the total energy conservation of a combined solid and liquid phases and by invoking the assumption that the local thermodynamic equilibrium prevails among two phases. The temperature of the RPP during unsaturated flow due to supplied hot water is obtained by solving the conventional heat transfer equation.

$$\begin{aligned} & \frac{\partial}{\partial t} [(\rho c)_T T] + \frac{\partial}{\partial z} [(\rho_l c_{pl} v_l) T] + \frac{\partial}{\partial x} [(\rho_l c_{pl} u_l) T] \\ &= \frac{\partial}{\partial z} \left[\lambda_{eff} \frac{\partial T}{\partial z} \right] + \frac{\partial}{\partial x} \left[\lambda_{eff} \frac{\partial T}{\partial x} \right] \end{aligned} \quad (3)$$

where $(\rho c)_T$ is the effective heat capacitance of porous layered, λ_{eff} is the effective thermal conductivity depending on water saturation. Under thermal equilibrium conditions and using the volume average technique, the effective heat capacitance is given by:

$$(\rho c_{pl})_T = \rho_l c_{pl} \varepsilon s + \rho_p c_{pp} (1 - \varepsilon) \quad (4)$$

where ε is porosity

Based on the experimental results [14, 15] using glass beads saturated with water, the effective thermal

conductivity is represented as a function of the water saturation:

$$\lambda_{eff} = \frac{0.8}{1 + 3.78e^{-5.95s}} \quad (5)$$

Equilibrium Relations

The system of conservation equations obtained for multiphase transport mode requires constitutive equation for relative permeability, K_r , capillary pressure, p_c and capillary pressure functions (Leverett functions), J . A typical set of constitutive relationships for liquid and gas system is given by:

$$K_{rl} = s_e^3, \quad K_{rg} = (1 - s_e)^3 \quad (6)$$

where s_e is the effective water saturation considered the irreducible water saturation, s_{ir} , and can be defined by [19]:

$$s_e = \frac{s - s_{ir}}{1 - s_{ir}} \quad (7)$$

The relationship between relative permeability in each phase following Eq. (6) is shown in Fig. 2

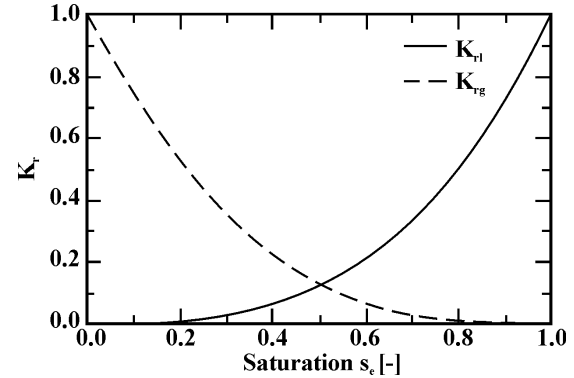


Fig. 2 The relationship between, K_r and s_e
[16]

The capillary pressure, p_c , is further assumed to be adequately represented by Leverett's well know $J(s_e)$ functions. The relationship between the capillary pressure and the water saturation is defined by using Leverett functions, $J(s_e)$ [16]

$$p_c = p_g - p_l = \frac{\sigma}{\sqrt{K/\phi}} J(s_e) \quad (8)$$

where σ is surface tension, $J(s_e)$ is correlated capillary pressure data obtained by Leverett and can be expressed follows:

$$J(s_e) = a(1/s_e - 1)^b \quad (9)$$

Further, the coefficients "a" and "b" at each condition, can be directly taken from reference [14].

CST0006

Initial Condition and Boundary Conditions

According to the Fig. 1 boundary conditions proposed for two-dimensional models with the dimensions of 15 cm (x) x 20 cm (z) are shown in Fig. 3. The initial conditions are given by uniform initial temperature and water saturation.

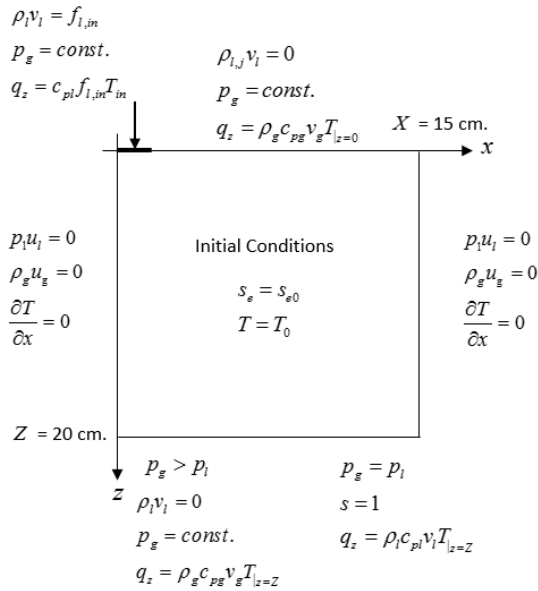


Fig. 3 Initial condition and boundary conditions of two-dimensional model

Initial condition and boundary conditions can be written as:

$$\begin{aligned}
 x=0, z=0 : \rho_l v_l = f_{l,in}, \quad p_g = p_g|_{z=0} = const., \quad q_{in} = c_{pl} f_{l,in} T_{in} \\
 x=0, z \geq 0 : \rho_l u_l = 0, \quad \frac{\partial T}{\partial x} = 0 \\
 x=X, z \geq 0 : \rho_l u_l = 0, \quad \frac{\partial T}{\partial x} = 0 \\
 x \geq 0, z=0 : \rho_l v_l = 0, \quad p_g = p_g|_{z=0} = const. \\
 x \geq 0, z=Z : \rho_l v_l = 0, \quad p_g = p_g|_{z=Z} = const. \\
 x \geq 0, z=Z, \quad \begin{cases} \rho_l v_l = 0, \quad p_g = p_g|_{z=Z} = const. \\ s = 1, \quad q_z = \rho_l c_{pl} v_l T|_{z=Z} \end{cases}
 \end{aligned} \quad (10)$$

3. Numerical Procedure

Corresponding to the method of finite differences based on the notion of control volumes, the generalized system of nonlinear equations are integrated over typical rectangular control volumes. After integrating over each control volume within the computational mesh, a system of nonlinear equations result, whereby each equation within this system can be cast into a numerical discretization of the generalized conservation equation. The equations of heat transfer and unsaturated flow are nonlinear because, p_c , K_{rl} and K_{rg} depend on s . To solve the nonlinear equations, the Newton-Raphson iteration procedure is used for each element.

4. Result and Discussion

Verification of the model

This study, the presented numerical results has been validated against the reference [22] result which was directly taken from the work of Akahori, M et al., [22]. The verification of the model is only picked up the value from a source points of a center line of porous domain ($x = 0$ cm, z) with 3 elapsed times as shown in Table. 1, where the testing conditions used are supplied water flux, $f = 0.15$ kg/m²s, supplied water temperature, $T_s = 50^\circ\text{C}$ and particle size of 0.15 mm. It is found that the fairly agreement of the infiltration front at 10, 20 and 30 min between Reference [22] and presented study is clearly shown.

Table. 1 The comparative results

Time [min]	Infiltration front [cm] ($x = 0$ cm, z)	
	Presented study	Reference [22]
10	12	10
20	14	12
30	17	14

Two-Dimensional Water Infiltration and Heat Transfer

This study described the dynamics of water infiltration and heat transfer in various condition. The particle sizes used in this work are 0.15 mm and 0.40 mm in diameter, supplied water fluxes is 0.15 kg/m²s supplied water temperature is controlled at 50°C and the initial temperature T_0 is given as $T_0 = 0^\circ\text{C}$.

Here, the main transport mechanism that enables water infiltration in granular packed bed is by capillary pressure gradient and gravity. Liquid phase migration is related to capillary pressure gradient as well as temperature (which correspond to that of surface tension, as referred to in Eq.8).

The two-dimensional water infiltration and heat transfer in x- and z-directions (the contour plot is based on symmetrical plan) will now be discussed with the aids of Figs. 4 - 7. Fig. 4 and Fig. 6 show the effect of particle size on the expansion of the heated layer due to infiltration of supplied hot water. The heated layer expands somewhat in the z-direction at a larger particle size, but the effect of particle size on the expansion of the heated layer is smaller as compared to the infiltration layer (Fig. 5 and Fig. 7). It is found that the heated layer are always wider in the z-direction and narrower in the x-direction for a larger particle size (Fig. 6).

Fig. 5 and Fig. 7 show the effect of particle size on water infiltration under a constant supplied water flux. In the early stage of infiltration, the infiltration layer expands uniformly in both x- and z-directions because capillary pressure has more influence than a gravity potential. As water infiltration progresses, the gravitational effect becomes superior to the capillary pressure and the infiltration layer expands wider in the z-direction which is the direction of gravity. However, the infiltration front in the case of small particle size

CST0006

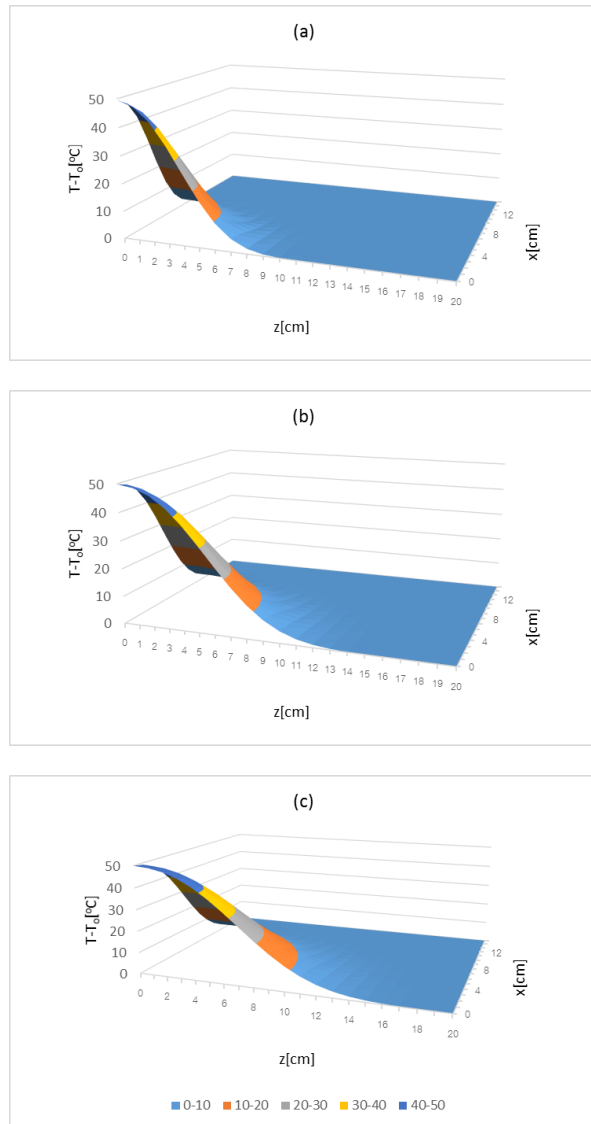


Fig. 4 The temperature distribution in RPP with particle size of 0.15 mm. when time at (a) 15 min, (b) 30 min and (c) 45 min

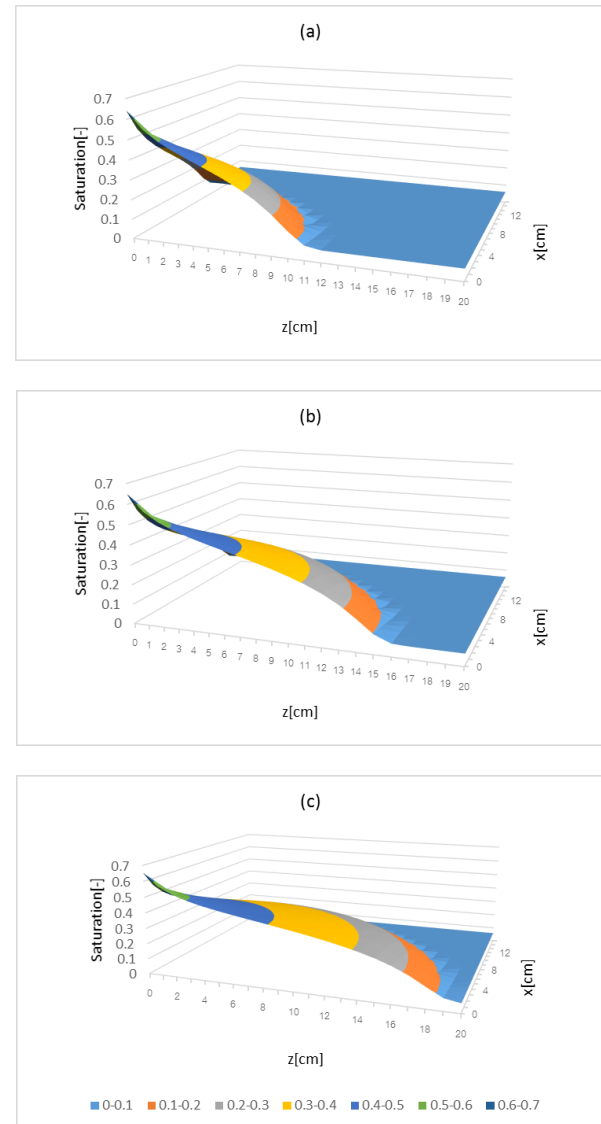


Fig. 5 The water saturation distribution in RPP with particle size of 0.15 mm. when time at (a) 15 min, (b) 30 min and (c) 45 min

expands wider in the x -direction in comparison with a larger particle size, due to the stronger effect of the capillary pressure.

Fig. 8, which redrawn from Figs. 4 - 7, shows the distributions of temperature and water saturation at the center line of RPP ($x = 0$) with various elapsed times as a parameter of particle sizes. It is found that a greater particle sizes corresponds to higher water saturation and forms a wider infiltration layer. The temperature in the granular packed bed rises due to water infiltration, but the heated layer does not extend as much as the infiltration layer similarly explained in previous figures. Fig. 9 and Fig. 10 shows the distributions of temperature and water saturation at various elapsed times as a parameter of particle sizes at the positions ($x, z = 5$) and ($x, z = 10$), respectively. From Fig. 9(a), it is found that the temperature distributions of both particle sizes taken at the early stage show nearly the same tendency, that is the temperature decreases to low values within short

distance in x direction. While in the later stages, the some different temperature between the two particles sizes occurs over an infiltration layer. This is because the permeability of the porous medium as well as the capillary pressure is become the weakly dominant factor to the water infiltration and heat transfer in the deeper location of granular packed bed during infiltration process. The result shows that a smaller particle size leads to faster infiltration rate and forms a wider infiltration layer in x -direction, especially at the times of 30s and 45s. This is because at the location where $z = 5$ cm is closed to the heated zone which the capillary action is still a dominant mode for smaller particle size. In addition, it is found that using the larger particle size results in lower water saturation at the location of $x = 0 - 6$ cm ($t = 15$ min) but it penetrates much deeper than that of the smaller particle size at $x = 6 - 11$ cm. This is because the larger particle size and hence pore size of these particles

CST0006

reduces the capillary pressure to resist a gravity driven during water infiltration process

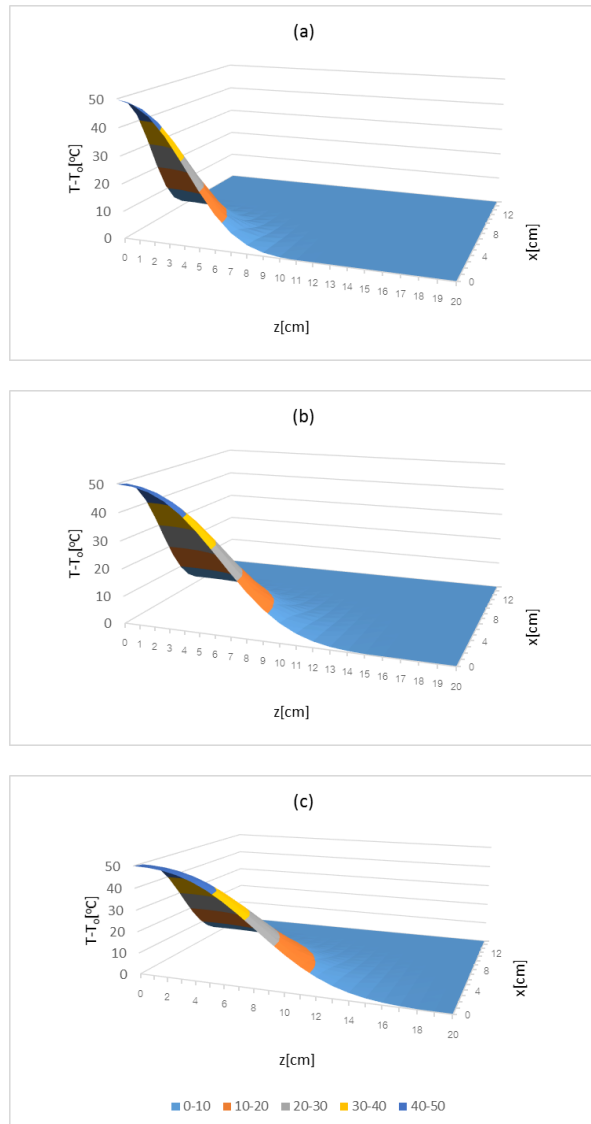


Fig. 6 The temperature distribution in RPP with particle size of 0.40 mm. when time at (a) 15 min, (b) 30 min and (c) 45 min

From Fig. 10(a) it is found that the temperature distributions of both particle sizes taken at the early stage show nearly the same tendency, that is the temperature decreases to low values in x-direction. While in the later stages, the significantly different temperature between the two particles sizes occurs over an infiltration layer where the larger particle size clearly displays a higher temperature. This is because the permeability of the porous medium as well as the gravitational force for case of larger particle size is become the strongly dominant factor to the water infiltration and heat transfer at the lower part of RPP ($z = 10$). Fig. 10(b), it is also found that using the larger particle size results in more penetrated deeper in x-direction than that of the smaller particle size at each time instant. Generally, this phenomenon is probably

caused by the type of head gradient that induced these water infiltration.

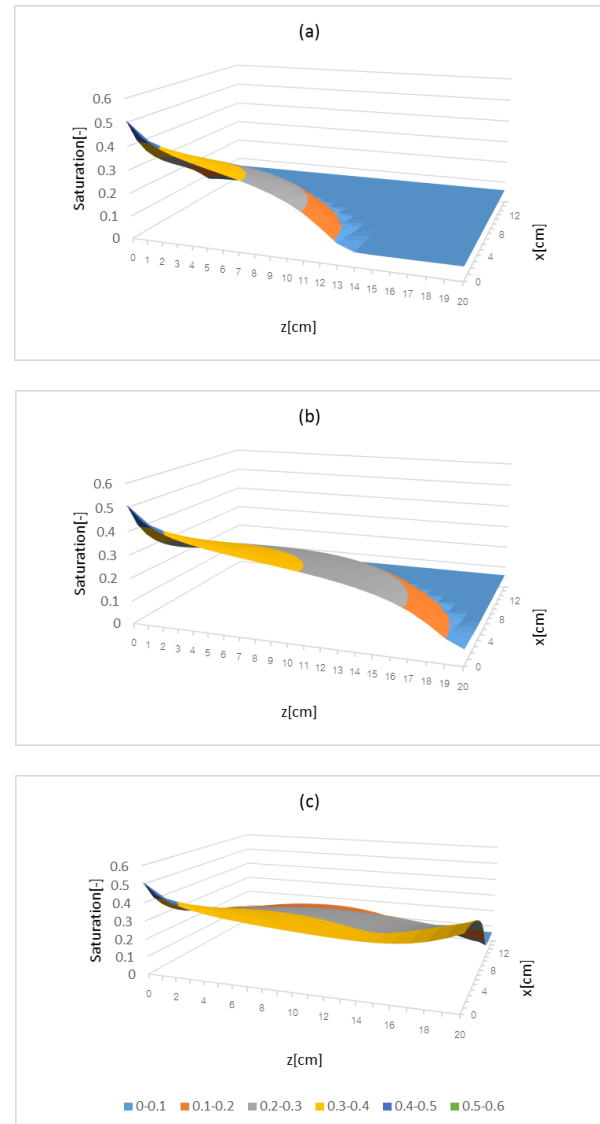


Fig. 7 The water saturation distribution in RPP with particle size of 0.40 mm. when time at (a) 15 min, (b) 30 min and (c) 45 min

The water infiltration of x-direction was achieved just by horizontal water movement, which is by the gradient in capillary tension only; while the water infiltration of z-direction was achieved by vertical water movement, which is by both gravity and the gradient in capillary tension.

CST0006

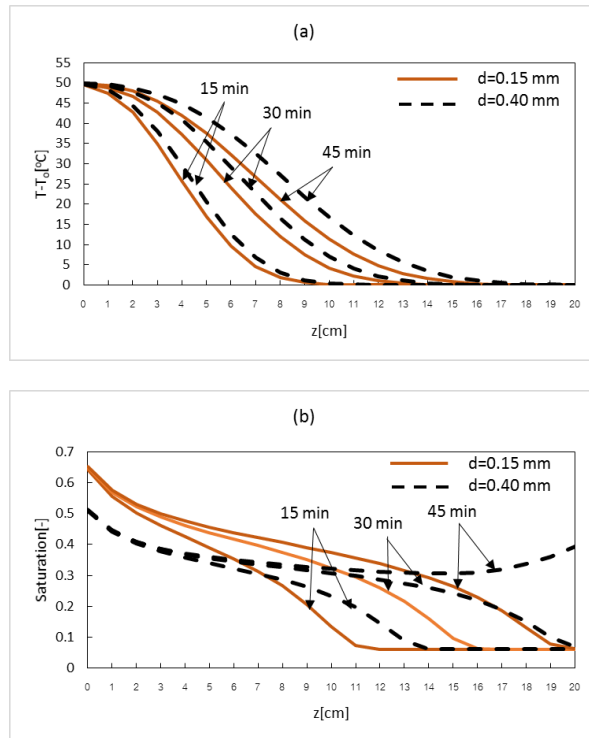


Fig. 8 Numerical results of (a) temperature profiles and (b) water saturation along z -direction of RPP with the particle sizes of 0.15 and 0.4 mm with respect to elapsed times. (Supplied water flux $f = 0.15 \text{ kg/m}^2\text{s}$, and supplied water temperature $T_s = 50^\circ\text{C}$.)
($x = 0 \text{ cm}$, z)

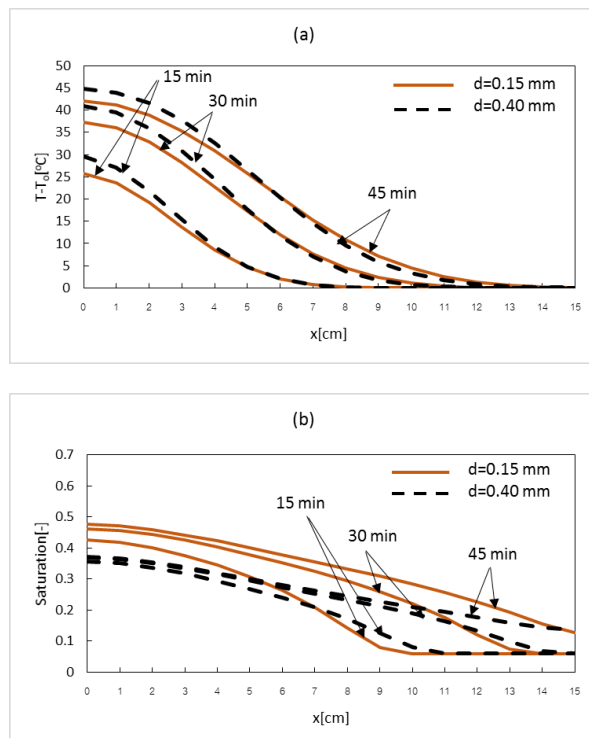


Fig. 9 Numerical results of (a) temperature profiles and (b) water saturation along x -direction of RPP with the particle sizes of 0.15 and 0.4 mm with respect to

elapsed times. (Supplied water flux $f = 0.15 \text{ kg/m}^2\text{s}$, and supplied water temperature $T_s = 50^\circ\text{C}$.)
($x, z = 5 \text{ cm}$)

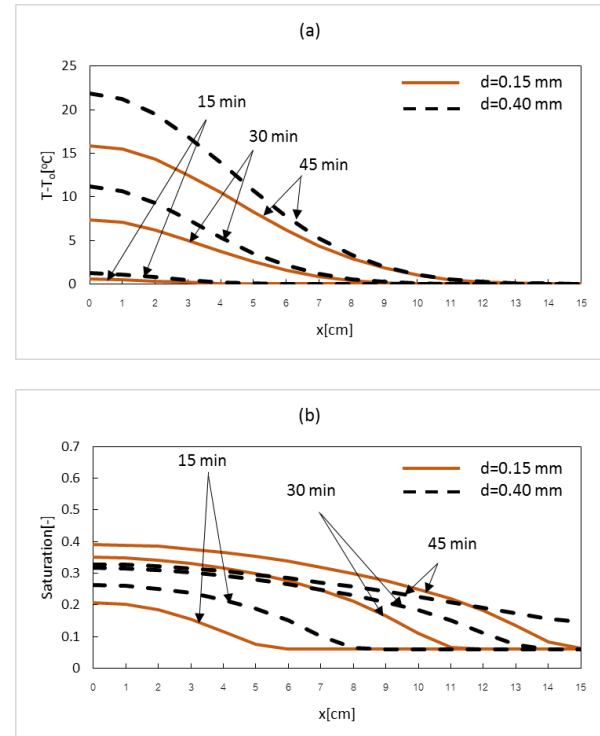


Fig. 10 Numerical results of (a) temperature profiles and (b) water saturation along x -direction of RPP with the particle sizes of 0.15 and 0.4 mm with respect to elapsed times. (Supplied water flux $f = 0.15 \text{ kg/m}^2\text{s}$, and supplied water temperature $T_s = 50^\circ\text{C}$.)
($x, z = 10 \text{ cm}$)

5. Conclusions

Based on two-dimensional models where there is thermal equilibrium between the water and the matrix at any specific space, the heat transfer in rectangular porous packed bed with unsaturated flow is investigated. The following are the conclusions of this work:

1) A generalized mathematical model of heat transfer with water infiltration within a granular packed bed is proposed. It is used successfully to describe the flow phenomena under various conditions.

2) When comparing the distribution profiles between heated layered and infiltration layer. It is observed that the heated layer does not extend as much as the infiltration layer. This means that heat transfer hardly occurs in the layer close to the infiltration front because the temperature of water infiltrating gradually drops, due to upstream heat transfer. Furthermore, the effect of particle size on the discrepancy of heated layers is smaller, compared to that of the saturation on infiltration layer.

CST0006

3) It is found that the gravity and capillary pressure have clearly exhibited influence on the infiltration and heat layers.

4) It is possible to use the present model for analysis of numerous other applications (e.g. heat and water movement in the ground).

6. Acknowledgement

The authors are pleased to acknowledge the Thailand Research Fund (Contract No. RTA 5980009) and Thammasat Ph.D. scholarship program for supporting this research work.

7. References

- [1] Campbell, G.S. (1985). Soil physics with basic, Elsevier, New York.
- [2] Bear, J. (1972). Dynamics of fluids in porous media, Elsevier, New York.
- [3] Haverkamp, R., Vauclin, M., Touma, J., Wierenga, P.J. and Vachaud, G. (1977). A comparison of numerical simulation models for one-dimensional infiltration, *Soil Sci. Soc. Am. J.*, Vol. 41, pp. 285-294.
- [4] Parlange, J.Y. (1972). Theory of water-movement in soils, one-dimensional infiltration. *Soil Sci*, Vol. 111, pp. 170-174.
- [5] Schrefler, B. A. and Zhan Xiaoyong. (1993). A fully coupled model for a water flow and air flow in deformable porous media, *Water Resources Research*, Vol. 29, pp.155-167.
- [6] Thomas, H.R., and King, S.D. (1991). Coupled temperature/capillary potential variations in unsaturated soil, *J. Engrg. Mech. ASCE.*, Vol. 117(11), pp. 2475-2491.
- [7] Thomas, H.R., and Sansom, M.R. Fully coupled analysis of heat, moisture, and air transfer in unsaturated soil, *J. Engrg. Mech. ASCE.*, Vol. 117(11), pp. 2475-2491.
- [8] Kutsovky, Y.E., Scriven, L.E., Davis, H.T., and Hammer, B.E. (1996). NMR imaging of velocity profiles and velocity distribution in packed beds, *Phy. Fluids*, Vol. 8, pp. 863.
- [9] Harlan, R.L. (1973). Analysis of coupled heat-fluid transfer in partially frozen soil, *Water Resources Research*, Vol. 9, pp. 1314-1323.
- [10] Kennedy, G.F., and Lielmezes, J. (1973). Heat and mass transfer of freezing water-soil systems, *Water Resources Research*, Vol. 9, pp. 395-400.
- [11] Guymon, G.L., and Luthin, J.N. (1974). A coupled heat and moisture transport model for arctic soils, *Water Resources Research*, Vol. 10, pp. 995-1001.
- [12] Ben Nasrallah, S., and Perre, P. (1988). Detailed study of a model of heat and mass transfer during convective drying of porous media, *Int. J. Heat and Mass Transfer*, Vol. 31, pp. 957-967.
- [13] Rogers, J.A., and Kaviani, M. (1992). Funicular and evaporative-front regimes in convective drying of granular beds, *Int. J. Heat and Mass Transfer*, Vol. 35, pp. 469-479.
- [14] Rattanadecho, P., Aoki, K., and Akahori, M. (2001). Experimental and numerical study of microwave drying in unsaturated porous material, *Int. Commun. Heat Mass Trans.*, Vol. 28, pp. 605-616.
- [15] Rattanadecho, P., Aoki, K., and Akahori, M. (2001). A numerical and experimental study of microwave drying using a rectangular wave guide. *Drying Technology International Journal*, Vol. 19, pp. 2209-2234.
- [16] Rattanadecho, P., Aoki, K., and Akahori, M. (2002). Influence of irradiation time, particle sizes and initial moisture content during microwave drying of multi-layered capillary porous materials, *ASME J. Heat Transfer*, Vol. 124, pp. 151-161.
- [17] Suttisong, S. and Rattanadecho, P. (2011). The experimental investigation of heat transport and water infiltration in granular packed bed due to supplied hot water from the top: influence of supplied water flux, particle sizes and supplied water temperature, *Int. J. Experimental Thermal and Fluid Science*, Vol. 35, pp. 1530-1534.
- [18] Suttisong, S., Rattanadecho, P. and Montienthong, P. (2013). Comparison of stefan model with single-phase model of water infiltration process in unsaturated porous media (theory and experiment), *Int. J. of Hydrology*, Vol. 497, pp. 145-151.
- [19] Rattanadecho, P., Suttisong, S. and Somtawin, T. (2014). The numerical and experimental analysis of heat transport and water infiltration in a granular packed bed due to supplied hot water, *Int. J. Numerical Heat Transfer, Part A*, Vol. 65, pp. 1007-1022.
- [20] Aoki, K., Hattori, M., Kitamura, M., and Shiraishi, N. (1991). Characteristics of heat transport in porous media with water infiltration, *ASME/JSME Thermal Eng. Proceeding*, Vol. 4, pp. 303-308.
- [21] Kaviani, M., and Mittal, M. (1987). Funicular state in drying of porous slab, *Int. J. Heat and Mass Transfer*, Vol. 30, pp. 1407-1418.
- [22] Akahori, M. Ph.D. Thesis, Nayaoka University of Technology, Japan.